Journal of Power Sources 196 (2011) 2773–2778

Contents lists available at ScienceDirect

Journal of Power Sources

journal homepage: www.elsevier.com/locate/jpowsour

Hydrogen production via urea electrolysis using a gel electrolyte

Rebecca L. King, Gerardine G. Botte*

Center for Electrochemical Engineering Research, Department of Chemical and Biomolecular Engineering, 165 Stocker Center, Ohio University, Athens, OH 45701, USA

ARTICLE INFO

Article history:
Received 13 September 2010
Received in revised form 2 November 2010
Accepted 3 November 2010
Available online 9 November 2010

Keywords:
Urea electrolysis
Urea electrolytic cell
On-board hydrogen production
Hydrogen storage
Fuel cells

ABSTRACT

A technology was demonstrated for the production of hydrogen and other valuable products (nitrogen and clean water) through the electrochemical oxidation of urea in alkaline media. In addition, this process remediates toxic nitrates and prevents gaseous ammonia emissions. Improvements to urea electrolysis were made through replacement of aqueous KOH electrolyte with a poly(acrylic acid) gel electrolyte. A small volume of poly(acrylic acid) gel electrolyte was used to accomplish the electrochemical oxidation of urea improving on the previous requirement for large amounts of aqueous potassium hydroxide. The effect of gel composition was investigated by varying polymer content and KOH concentrations within the polymer matrix in order to determine which is the most advantageous for the electrochemical oxidation of urea and production of hydrogen.

1. Introduction

1.1. Hydrogen production and reduction of ammonia emissions

The success of the hydrogen economy requires a safe, efficient, and environmentally friendly method for hydrogen production. Standard methods for hydrogen production generate substantial green house gases (steam reforming) or require significant electrical energy input (water electrolysis). The electrochemical oxidation of urea to hydrogen in alkaline media has significant benefits over standard hydrogen production methods. Pure hydrogen (100%) is produced at low temperature, pressure, and energy consumption along with other valuable products, such as nitrogen (96.1%) and clean water [1].

Urea-rich wastewater is widely abundant and currently purged into rivers and lakes where it undergoes a natural conversion to ammonia. Ammonia is then released in the gas phase to Earth's atmosphere resulting in billions of dollars in health costs each year [2]. Current methods for wastewater denitrification are expensive and time-consuming [3]. Electrolysis of urea remediates nitrate contamination in ground and drinking water, which is regarded as an epidemic by the U.S. Environmental Protection Agency [4]. Therefore, urea electrolysis offers multiple benefits with the direct conversion of urea to valuable hydrogen, which has not been accomplished with any other technology to date [5–7]. As shown in the proposed mechanism [1], urea is oxidized at the anode at a standard theoretical potential of −0.46 V vs. the standard hydrogen electrode (SHE) (Eq. (1)) with a competing nickel catalyst oxidation that occurs at 0.49 V vs. SHE (Eq. (2)). Water is reduced at the cathode at −0.83 V vs. SHE (Eq. (3)) to give an overall theoretical potential of 0.37 V at standard conditions (Eq. (4)). In-depth studies on reaction mechanisms of urea electrolysis are continuing to be investigated at the Center for Electrochemical Engineering Research at Ohio University. Results will be published in the future as they will be relevant for future development and implementation of the technology.

$$CO(NH_2)_{2(aq)} + 6OH^- \rightarrow N_{2(g)} + 5H_2O_{(l)} + CO_{2(aq)} + 6e^- \quad (1)$$

$$Ni(OH)_{2(s)} + OH^- \rightarrow NiOOH_{(s)} + H_2O_{(l)} + e^- \quad (2)$$

$$6H_2O_{(l)} + 6e^- \rightarrow 3H_{2(g)} + 6OH^-_{(aq)} \quad (3)$$

$$CO(NH_2)_{2(aq)} + H_2O_{(l)} \rightarrow N_{2(g)} + 3H_{2(g)} + CO_{2(aq)} \quad (4)$$

It has been demonstrated that inexpensive nickel is the most active catalyst for the electrochemical oxidation of human urine in alkaline media [1,8], which consists of 0.33 M urea [9]. Nickel oxide electrodes are active electrocatalysts for the oxidation of many organic compounds [10]. In basic solution, nickel exists in both divalent and trivalent states on the surface of a nickel oxyhydroxide modified nickel electrode (NOMN) (Eq. (2)). However, the nickel oxide layer is not stable, and the active nickel oxide (NiOOH) sites are consumed as the organic compound is oxidized [10,11]. Several methods of activation have successfully increased the amount of the active form [11–13].

The electrolyte currently used in urea electrolysis is aqueous KOH. The use of gel electrolyte would present a significant improvement for the process by eliminating the need for aqueous KOH

* Corresponding author. Tel.: +1 740 593 9670; fax: +1 740 593 0873.
E-mail address: botte@ohio.edu (G.G. Botte).

0378-7753/$ – see front matter © 2010 Elsevier B.V. All rights reserved.
doi:10.1016/j.jpowsour.2010.11.006

resulting in a system that is cheaper, safer, easier to contain, and more adaptable to portable applications. The KOH would be contained in a smaller volume of gel electrolyte stored directly between the electrodes as compared to aqueous electrolyte which requires distribution throughout the entire waste stream. The additional step of KOH recovery is then eliminated which further reduces cost.

1.2. Gel electrolyte

Solid polymer electrolytes have long been of interest for application in batteries because they are safer, more flexible, and easier to contain than their aqueous counterparts [14–16]. Leakage of the corrosive alkaline solution contained in batteries presents a hazard, and has made it desirable to find a solid polymer electrolyte (SPE) to substitute. Alkaline polymer electrolytes provide many advantages over their traditional liquid or solid alternatives [17], but in order to replace aqueous electrolytes, the SPE must have an ionic conductivity on the order of 10^{-2} S cm^{-1} as well as good mechanical, chemical and electrochemical stability [14–18].

In an effort to enhance conductivity, polymer gel electrolytes (PGEs) have been explored more recently. Polymer gel electrolytes entrap the aqueous alkaline electrolyte inside the polymer matrix, giving conductivities of 0.5–10^{-3} S cm^{-1}. These PGEs tend to have a higher conductivity but lower mechanical integrity and stability than SPEs [17]. Cross-linking agents and increased polymer content can be implemented with the gel-type electrolytes in order to increase stability and mechanical strength.

Polyethylene oxide (PEO) was amongst the first polymer to be recognized as a feasible candidate as gel electrolyte [19,20]. A system of PEO/KOH/H_2O has been used in rechargeable batteries such as Ni–Cd, Ni–Zn, Ni–MH with a conductivity of 10^{-3} S cm^{-1} [21–23].

Aside from battery and fuel cell applications, gel electrolytes could also be used in electrolytic cells to replace aqueous electrolytes. For example, polymer electrolytes have been applied in electrolysis of formic acid, ammonia, halogen acids (HCl, HBr), and water using Nafion membrane electrolytes [24–29].

Poly(acrylic acid) (PAA) cross-linked polymer is well-known to have high water absorbing capacity, gel strength, and low cost with a facile preparation [17]. The PAA gel investigated here was a poly(acrylic acid–KOH–H_20) matrix known to provide high conductivity of 0.6 S cm^{-1} [30]. Like most other gel electrolytes, the PAA system still suffers from issues such as gel swelling and electrolyte loss through diffusion. This gel was optimized for urea electrolysis by varying the KOH concentration and PAA wt% in the polymer matrix in order to find the optimal combination of mechanical strength and electrochemical performance.

1.3. Objectives of the study

Within this context, the focus of this paper was the electrooxidation of urea utilizing a gel electrolyte to exploit its advantages (increased safety, flexibility, and volume requirement) over its aqueous counterpart. The goal was to determine an optimal composition which maximized mechanical strength and electrochemical performance of the PAA gel electrolyte and its feasibility in a urea electrolytic system. The three main objectives are as follows:

1. Demonstrate that PAA gel electrolyte can replace aqueous KOH for urea electrolysis.
2. Evaluate the performance of PAA gels in a urea electrolytic cell.
3. Evaluate different electrolyte compositions by varying KOH concentration and PAA wt% (2.00–8.00 M KOH and 5–25 wt% PAA). The electrochemical and chemical performance of the electrolytic cell was determined and mechanical strength and conductivities for synthesized gels were measured.

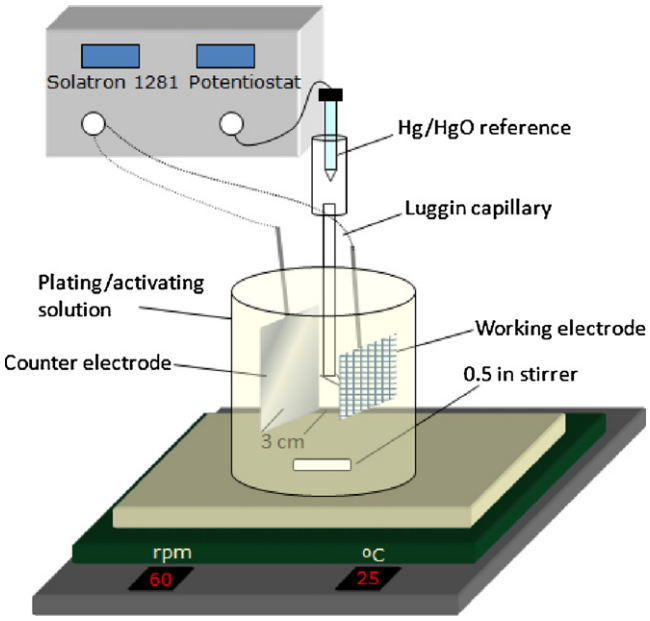

Fig. 1. Experimental setup for electrodeposition of platinum and activation of nickel substrate.

2. Experimental/materials and methods

2.1. Electrode preparation

Nickel gauze anodes were constructed by spot-welding titanium wire (Alfa Aesar, 99.99%, 1.0 mm diameter) to 6.25 cm^2 nickel gauze (Alfa Aesar, 100 mesh woven from 0.1 mm diameter wire). The nickel gauze was sandblasted and rinsed thoroughly with distilled water followed by activation of the nickel surface (see Section 2.3). Cathodes were prepared by electroplating platinum on this nickel gauze substrate.

2.2. Electrodeposition

The experimental setup for electrodeposition is depicted in Fig. 1. Platinum counter electrodes were made by deposition of platinum at 25 °C from an alkaline bath consisting of 3 M sodium hydroxide (Fisher 99.5%) and 2.4 g L^{-1} dihydrogen hexachloroplatinate (IV) hexahydrate (Alfa Aesar 99.9%) solvated with ultrapure water (Alfa Aesar, HPLC grade). A Solartron 1281 multiplexer potentiostat was used to deposit platinum with a loading of 0.60 ± 0.02 mg cm^{-2} potentiostatically at −0.60 V vs. Hg/HgO reference electrode equipped with a Luggin capillary and a platinum foil counter electrode (Sigma Aldrich, 0.05 mm thick 99.99%) with stirring at 60 rpm.

2.3. Activation

Various methods have been described for activating a nickel electrode to a more active NiOOH form [11–13]. Nickel gauze electrodes used in this study were activated by cycling the nickel gauze from 0.20 to 0.58 V vs. Hg/HgO (experimental setup same as Fig. 1) to exploit the region in which the $Ni(OH)_2$ to NiOOH transition occurs. Sweeps were performed at 15 mV s^{-1} for 20 cycles in 1 M KOH (Fisher) with a platinum-coated nickel gauze counter electrode (0.6 mg cm^{-2}, 6.25 cm^2).

Table 1
Experimental matrix for electrolyte preparation.

Batch	KOH (M)	PAA (wt%)
1	8.00	7.0
	6.00	7.0
	4.00	7.0
	2.00	7.0
2	5.00	15.0
	5.00	10.0
	5.00	5.0
3	8.00	25.0
	8.00	20.0
	8.00	15.0
	8.00	10.0

2.4. Electrolyte preparation

The experimental matrix of synthesized gel compositions is summarized in Table 1. Variations of PAA gel were prepared with 5.0–15.0 ± 0.1 wt% PAA at a constant KOH concentration of 5.00 ± 0.04 M (Batch 1) and 2.00–8.00 M KOH with a constant PAA content of 7.0 ± 0.1 wt% (Batch 2). The gels were synthesized by dissolving the appropriate amount of PAA partial potassium salt (Sigma Aldrich, lightly crosslinked) in 250 mL of 2.00–8.00 M KOH to give 5–15 wt% PAA. Each solution was stirred for 30 s, covered with parafilm, and allowed to stand for three days, at which point the gel was placed in a vacuum chamber (Napco 5831) and held under vacuum for 48 h (Duniway Stockroom Corp, model no. 29476-5, 29 mmHg) [30]. The optimum KOH concentration as determined from this initial investigation of compositions was then used to formulate another batch of gels with higher polymer content ranging from 15 to 25 wt% (Batch 3) in an attempt to enhance the mechanical integrity of the gel. Batch 3 was synthesized according to the same procedure except with 100 mL of 8 M KOH to dissolve the PAA salt (Table 1). Aqueous KOH electrolyte (1 M) was used for comparison of gel performance.

2.5. Electrolyte evaluation

A cell was designed for electrolyte comparisons that allowed the gel to contact the catalytic material without directly contacting the electrolysis solution (Fig. 2). An acrylic spacer held the gel at a consistent thickness of 0.3 cm between the surfaces of the activated nickel gauze anode and platinum cathode. Acrylic plates were then attached on both ends with Teflon screws to secure the electrode/gel assembly. Each gel was tested via cyclic voltammetry (CV) from 0.0 to 0.8 V vs. Hg/HgO and with constant cell voltage of 1.54 V in the presence and absence of 0.33 M urea (Fisher 99.8%) by placing this apparatus in an open beaker as shown in Fig. 3. This device was used for electrochemical testing with both the aqueous and gel electrolytes to ensure consistency where all gels were tested with no KOH in the surrounding aqueous phase. The cell voltage for constant voltage testing was chosen based on cathodic and anodic CV sweeps (0.0 to −1.0 V and 0.0–0.8 V vs. Hg/HgO) with the reference on the nickel and platinum electrodes, respectively, in conjunction with constant voltage testing in the range of 1.40–1.56 V in 1 M KOH aqueous electrolyte and 0.33 M urea to determine where urea electrolysis was maximized with negligible water electrolysis. All CVs were performed using a Luggin capillary filled with 1 M KOH to support the reference electrode and consisted of three cycles where the third pseudo-steady state cycle is reported.

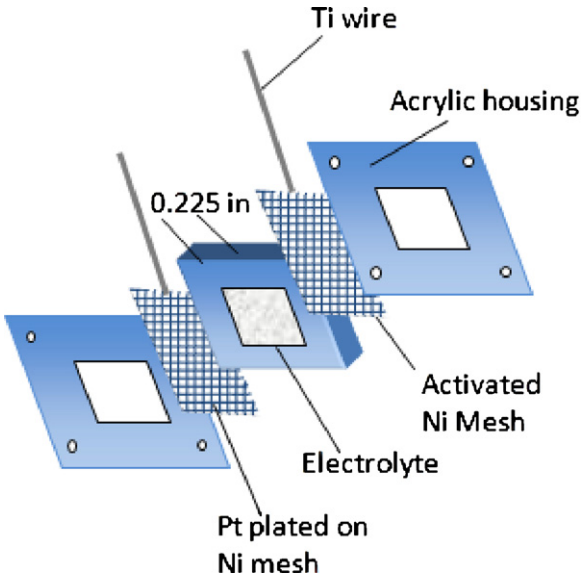

Fig. 2. Acrylic cell assembly designed for gel testing.

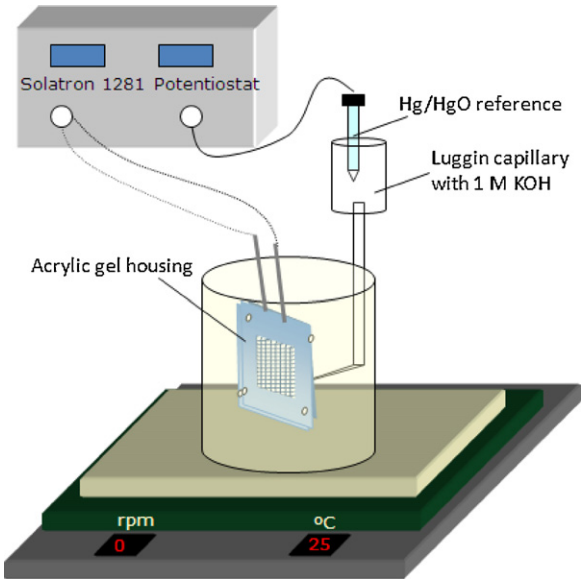

Fig. 3. Experimental setup for electrochemical evaluation of urea oxidation using acrylic gel testing assembly.

The conductivity of each gel was measured using electrochemical impedance spectroscopy (EIS) in a control potential (0 V), sweep frequency (100,000 Hz–10 Hz) experiment with 50 mV ac signal strength. The gels were held outside of solution in the acrylic assembly (Fig. 2) for the duration of EIS analysis. The cell constant (c) was first calculated to account for the physical configuration of the cell and electric field pattern fringe effects between the electrodes which affects the overall electrode area. This was done by measuring the resistance (R) of 0.01, 0.1, and 1.0 M KCl standard solutions of known conductivity (k) and calculating the cell constant as $c = k \times R$. The conductivity of each gel was then calculated as $k = c/R$ where R was taken as the high frequency intercept on the Nyquist plot in Fig. 4.

Electrolyte retention was studied by monitoring the pH of a constant volume of each gel (2.2 cm length × 2.2 cm width × 0.3 cm thick) submerged in 50 mL of distilled water. The pH was recorded with time for each gel over a period of 40 min to determine the amount of KOH that diffused out of the polymer matrix.

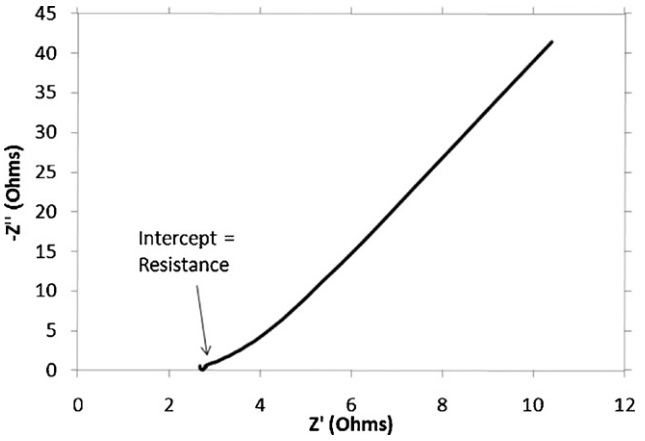

Fig. 4. Typical Nyquist plot of control potential (0 V), sweep frequency (100,000 Hz–10 Hz) impedance spectroscopy experiment used to determine the conductivity of each gel electrolyte variation.

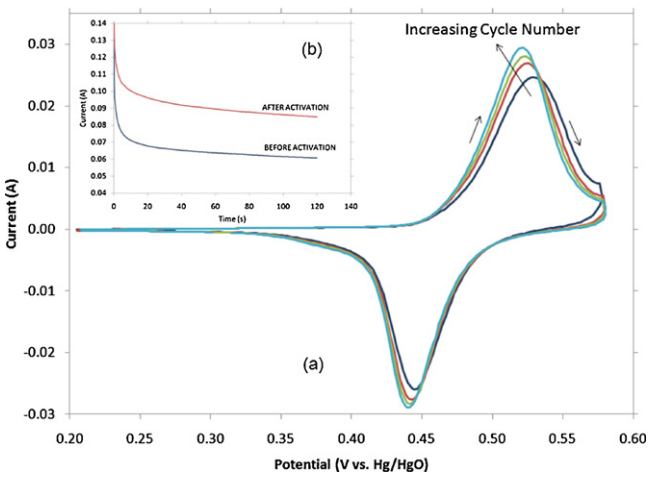

Fig. 5. Effect of activating of nickel anodes: (a) activation cycles from 0.20 to 0.58 V vs. Hg/HgO in 1 M KOH at 15 mV s^{-1} for 20 cycles, platinum foil counter electrode. (b) Constant voltage testing at 1.54 V in 1 M KOH and 0.33 M urea before and after activation.

3. Results and discussion

3.1. Activation

Fig. 5a shows the activation of the nickel surface via potential cycling as described in Section 2.3. The peak currents for NiOOH formation increased as these cycles progressed indicating successful generation of the active nickel form. Fig. 5b shows constant voltage testing at 1.54 V vs. cell in 1 M KOH and 0.33 M urea before and after activation. The cell current increased by nearly 50% after activation and thus indicates success of the technique.

3.2. Optimal cell voltage for urea electrolysis

The reactions at both anode (Eqs. (1) and (2)) and cathode (Eq. (3)) can be seen via a CV sweep in both the positive and negative potential regions in Fig. 6a. The dashed curve reveals a small peak in the absence of urea at 0.45 V vs. Hg/HgO, which is due to the transformation of Ni^{2+} to Ni^{3+} [10]. The curve in the presence of urea shows a significantly higher current than background KOH, which confirms the oxidation of urea is occurring. The peak for urea oxidation commences at the same potential as the nickel transformation indicating that urea is in fact being oxidized by the Ni^{3+} form. The peak upon forward scanning occurs due to consumption of active oxide sites. Water oxidation is evident as the potential is increased beyond 0.70 V vs. Hg/HgO. On the reverse scan, a sharp peak is observed at 0.68 V vs. Hg/HgO due to desorption of species from the electrode surface.

The anodic scan displays an appreciable current for urea oxidation in the region of 0.45–0.60 V vs. Hg/HgO with no appreciable water oxidation, whereas the cathodic sweep exhibits an appreciable current for water reduction from 0.95 to −1.0 V vs. Hg/HgO. The anodic and cathodic half-cell potentials sum to a total range of 1.40–1.60 V cell voltage to affect the oxidation of urea.

The cell was tested at constant voltages in the range of 1.40–1.56 V in 1 M KOH and 0.33 M urea to determine the fraction of the cell current due to the electrolysis of urea as shown in Fig. 6b. The dashed curves in all figures throughout this text represent 1 M

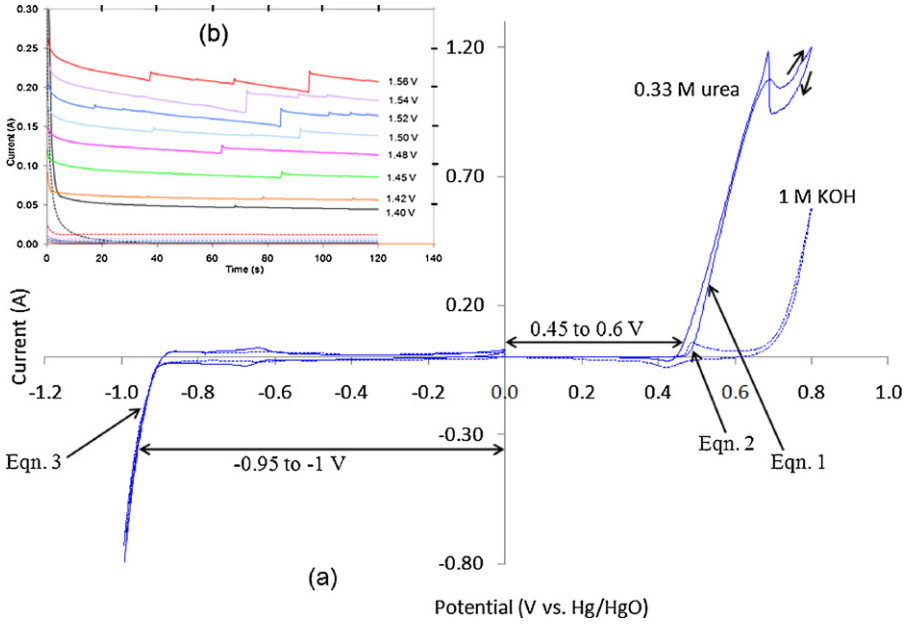

Fig. 6. (a) Combined CV with cathodic and anodic sweeps from −1.0 to 0.8 V in 1 M KOH and 0.33 M urea solutions, 10 mV s^{-1}. The dashed line represents KOH only. (b) Potentiostatic analyses from 1.40 to 1.56 V cell potential with Ni/C anode and Pt foil cathode in 1 M KOH and 0.33 M urea.

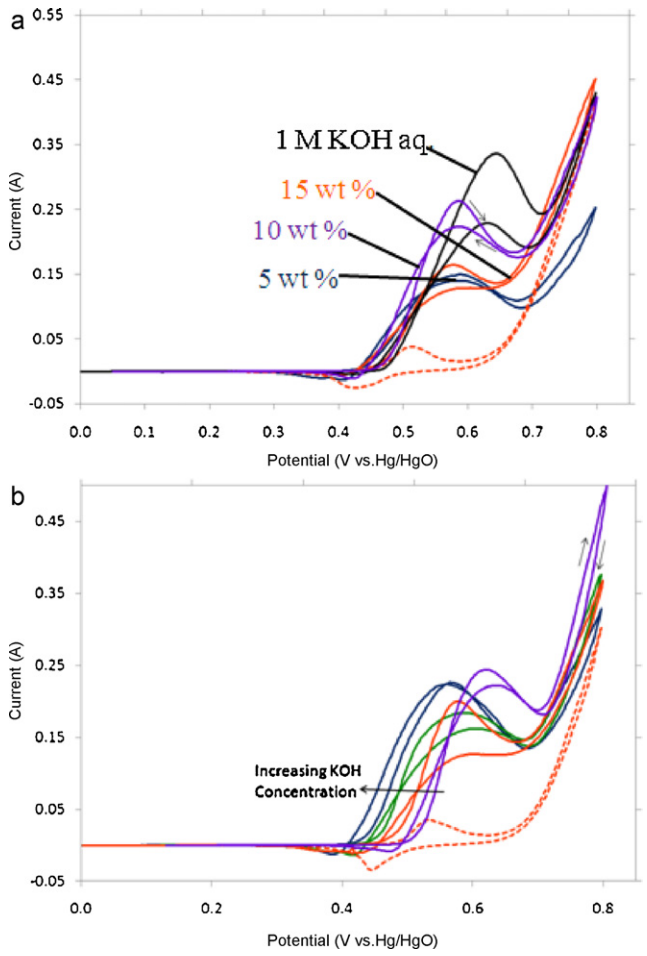

Fig. 7. CV comparison of PGEs from 0 to 0.8 V vs. Hg/HgO, 10 mV s^{-1} in 0.33 M urea: (a) Batch 1 and (b) Batch 2. Dashed lines represent 1 M aqueous KOH in the absence of urea.

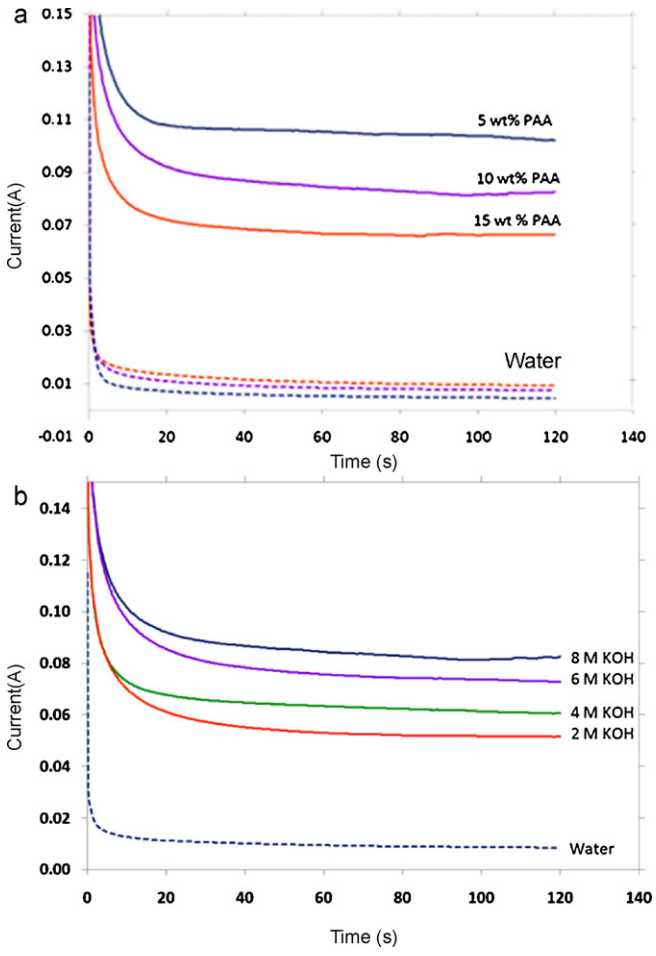

Fig. 8. Constant voltage comparison of PGEs at 1.54 V and 0.33 M urea solutions where dashed lines represent no urea: (a) Batch 1 and (b) Batch 2. Dashed lines represent 1 M aqueous KOH in the absence of urea.

aqueous KOH in the absence of urea. Sharp peaks were observed due to the release of gas collected on the electrode surface. All potentials in this range provide a significant current for urea electrolysis and the current increases steadily between each potential step, as expected. However, the percentage of current contributed by water electrolysis doubled from 10 to 20 mA as the voltage was stepped from 1.54 to 1.56 V. Therefore, 1.54 V was chosen for the remaining constant voltage experiments

3.3. *Electrolyte comparison*

Fig. 7a shows the cyclic voltammograms of each gel in Batch 1, which revealed a similar oxidation peak as compared with the aqueous electrolyte confirming that all gel compositions do in fact accomplish urea oxidation. The absence of additional peaks in the gel voltammograms indicates that all electrolytes are electrochemically stable in this potential region, regardless of the polymer content. Similar Batch 2 voltammograms shown in Fig. 7b revealed that increasing KOH concentrations provide an earlier onset of current for urea oxidation and are therefore more thermodynamically favorable because slightly lower potentials are required to initiate the reaction. For example, urea oxidation is initiated at 0.47 V vs. Hg/HgO for the 8 M KOH gel in comparison to 0.52 V vs. Hg/HgO required to initiate the reaction for the 2 M KOH gel.

Constant voltage analyses presented in Fig. 8 demonstrated that the current for urea electrolysis increases with KOH concentration and decreases with polymer content. Both batches demonstrate a minimal current for water electrolysis (dashed curve). However, it should be noted that a qualitative increase in mechanical strength was observed in gels with higher polymer content.

Fig. 9 presents the conductivity of each gel as a function of KOH concentration as determined from impedance spectroscopy. The results indicate that higher concentrations of KOH in the polymer matrix enhance conductivity while higher PAA content decreases

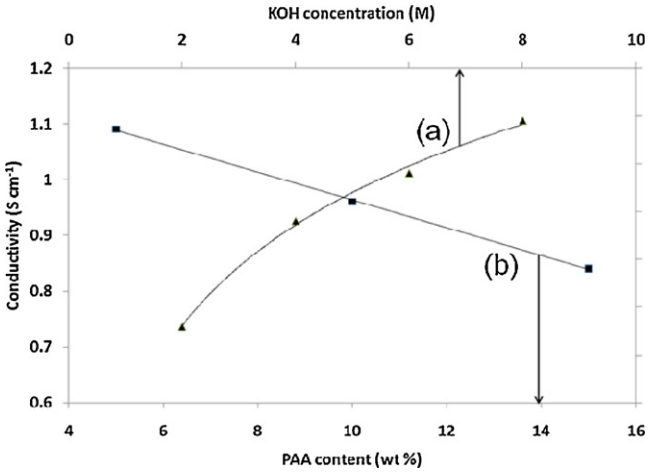

Fig. 9. Conductivity as measured from impedance spectroscopy: (a) Batch 1 and (b) Batch 2.

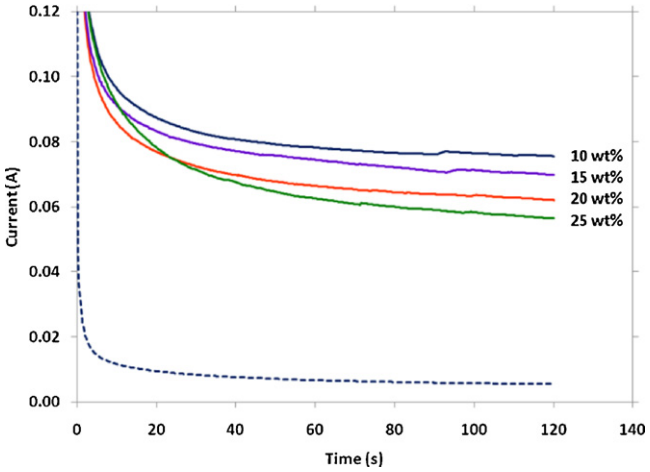

Fig. 10. Constant voltage analysis of Batch 3 PGEs at 1.54 V. Dashed line represents 1 M aqueous KOH in the absence of urea.

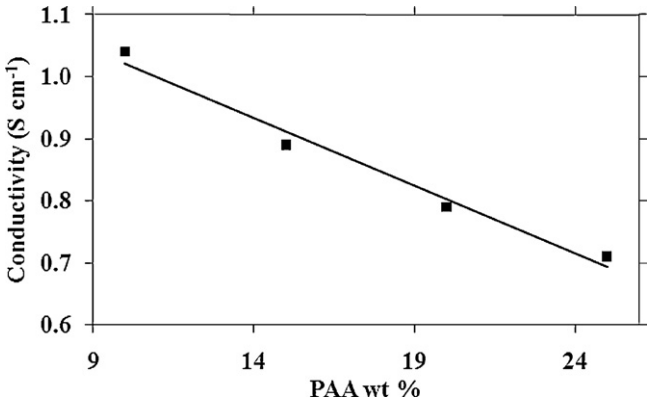

Fig. 11. Conductivity of Batch 3 PGEs as determined from impedance spectroscopy.

conductivity. Based on these outcomes from Batches 1 and 2, Batch 3 gels were synthesized with 8 M KOH and higher PAA content (10–25 wt%) in an attempt to enhance mechanical integrity while maintaining conductivity and activity for urea electrolysis.

Figs. 10 and 11 show that Batch 3 gels displayed similar trends of decreasing current in constant voltage analysis and decreasing conductivity with increasing PAA wt%. However, gels with higher PAA content better maintained shape and structure before and after electrolysis. The decrease in current was relatively small (less than 2 mA per 1 wt% PAA) when considering the increased mechanical integrity. Also, all gels in Batch 3 provided a higher conductivity ($0.70–1.05 \pm 0.02\ S\ cm^{-1}$) than 1 M aqueous electrolyte ($0.58\ S\ cm^{-1}$) despite the higher polymer content. Although the gels with higher PAA content displayed higher mechanical stability, gels did not congeal homogeneously beyond 25 wt%, which provided the upper limit for synthesis.

The KOH retention of each gel in Batch 3 was calculated by monitoring pH change in a known volume of solution after 24 h. This confirmed that all gels retained greater than $90 \pm 1\%$ of the original KOH in the polymer matrix and higher PAA wt% provided enhanced retention (10, 15, 20, and 25 wt% retained 90, 92, 93, and 94%, respectively.)

4. Conclusions

Replacement of KOH electrolyte with a gel electrolyte for hydrogen production through urea electrolysis would allow the process to be applicable for portable, distributed or remote hydrogen generation applications due to the inherent safety of the system. The gel electrolyte investigated here proved to be a viable option to replace aqueous KOH for urea electrolysis. Higher KOH concentration and lower polymer content provided higher current for urea electrolysis and higher conductivity. Of the gels examined, 8 M KOH and 15 wt% PAA was determined to be ideal for urea electrolysis. This 15 wt% variation provided the highest mechanical strength, ease of homogeneous preparation, and conductivity with only a slight compromise in current performance and electrolyte retention. It has also been shown that the nickel catalyst can be activated quickly and efficiently by cycling the potential in a region where divalent to trivalent nickel transition occurs. Together, these innovations have made urea electrolysis a more feasible means for hydrogen production, through waste remediation.

Acknowledgements

The authors would like to thank the financial support of the Chemical and Biomolecular Engineering Department at Ohio University and the Department of Defense through the U.S. Army Construction Engineering Research Laboratory (W9132T-09-1-0001). The content of the information does not reflect the position or the policy of the U.S. government.

References

[1] B. Boggs, R. King, G. Botte, Chem. Commun. 32 (2009) 4859–4861.
[2] D. McCubbin, B. Apelberg, S. Roe, Environ. Sci. Technol. 36 (2002) 1141–1146.
[3] C. Alfafara, T. Kawamori, N. Nomura, M. Kiuchi, M. Matsumura, J. Chem. Technol. Biotechnol. 79 (2004) 291–298.
[4] D. Bouchard, W. Mary, R. Surampalli, J. Am. Waste Water Assoc. 84 (1992) 85–90.
[5] K. Rittstieg, K. Robra, W. Somitsch, Appl. Microbiol. Biotechnol. 56 (2001) 820–825.
[6] J. Canfield, Research on Applied Bioelectrochemistry, Quarterly Progress Report No. 2, Magna Corporation NASw-623, 1963.
[7] H. B. H. Cooper, I. Spencer, W. Herbert, U.S. Patent 6 077 491 (2000).
[8] G. G. Botte, U.S. Patent 60 980 056 (2007).
[9] Urine, Brittanica Online Encyclopedia, 2007, http://www.britannica.com/EBchecked/topic/619857/urine.
[10] H.J. Schafer, Top. Curr. Chem. 142 (1987) 101–129.
[11] A. Vaze, S. Sawant, V. Pangarkar, J. Appl. Electrochem. 27 (1997) 584–588.
[12] Q. Yi, W. Huang, J. Zhang, X. Liu, L. Li, J. Electroanal. Chem. 610 (2007) 163–170.
[13] A. Kowal, S. Port, R. Nichols, Catal. Today 38 (1997) 483–492.
[14] G. Appetecch, F. Croce, P. Romagnoli, B. Scrosati, U. Heider, R. Oesten, Electrochem. Commun. 1 (1999) 83–86.
[15] W. Meyer, Adv. Mater. 10 (1998) 439–448.
[16] J. Song, Y. Wang, C. Wan, J. Power Sources 77 (1999) 183–197.
[17] X. Zhu, H. Yang, Y. Cao, X. Ai, Electrochim. Acta 49 (2004) 2533–2539.
[18] S. Sang, J. Zhang, Q. Wu, Y. Liao, Electrochim. Acta 52 (2007) 7315–7321.
[19] M. Armand, Solid State Ionics 69 (1994) 309–319.
[20] D. Fenton, J. Parker, P. Wright, Polymer 14 (1973) 589.
[21] E. Salmon, S. Guinot, J.F. Fauvarque, J. Appl. Polym. Sci. 65 (1997) 601.
[22] J. Fauvarque, S. Guinot, N. Bouzir, E. Salmon, J. Penneau, Electrochim. Acta 40 (1995) 2449.
[23] S. Guinot, E. Salmon, J. Penneau, J. Fauvarque, Electrochim. Acta 43 (1998) 1163.
[24] E. Kilic, A. Koparal, U. Ogutveren, Fuel Process. Technol. 90 (2009) 158–163.
[25] P. Choi, D. Bessarabov, R. Data, Solid State Ionics 175 (2004) 535–539.
[26] H. Cheng, K. Scott, P. Christensen, Chem. Eng. J. 108 (2005) 257–268.
[27] E. Rasten, G. Hagen, R. Tunold, Electrochim. Acta 48 (2003) 3945–3952.
[28] H. Takenaka, E. Torikai, Y. Kawami, N. Wakabayashi, Int. J. Hydrogen Energy 7 (1982) 397–403.
[29] E. Balko, J. McElroy, A. LaConti, Int. J. Hydrogen Energy 6 (1981) 577–587.
[30] C. Iwakura, S. Nohara, N. Furukawa, H. Inoue, Solid State Ionics 148 (2002) 487–492.